Journal of
Mechanics of
Materials and Structures

A HIGH-ORDER THEORY FOR CYLINDRICAL SANDWICH SHELLS WITH FLEXIBLE CORES

Renfu Li and George Kardomateas

Volume 4, Nº 7-8 September 2009

mathematical sciences publishers

JOURNAL OF MECHANICS OF MATERIALS AND STRUCTURES
Vol. 4, No. 7-8, 2009

A HIGH-ORDER THEORY FOR CYLINDRICAL SANDWICH SHELLS WITH FLEXIBLE CORES

RENFU LI AND GEORGE KARDOMATEAS

This paper presents a nonlinear high-order theory for cylindrical sandwich shells with flexible cores, extending a previously presented high-order theory for sandwich plates. The outer and inner faces are assumed to be relatively thin compared to the core and the effects from the core compressibility are addressed in the solution by incorporating the extended nonlinear core theory into the constitutive relations of the cylindrical shells. The governing equations and boundary conditions for the cylindrical shells are derived using a variational principle. Numerical results are presented for the cases where the two faces and the core are made of orthotropic materials. These results show that this model could capture the nonlinearity in the transverse stress distribution in the core of the cylindrical sandwich shell. Numerical results are presented on the details of the stress and displacement profiles for a cylindrical sandwich shell under localized external pressure. This study could have significance for the optimal design of advanced cylindrical sandwich shells.

1. Introduction

Unique properties such as high stiffness/weight and strength/weight ratios present increasing promise for applications of cylindrical sandwich shells in aerospace and marine vehicles, such as aircraft fuselage sections, rockets and submarine hulls. A cylindrical sandwich shell consists of outer and inner stiff thin faces made either from homogeneous metallic materials or composite laminates, separated by a thick core of soft foam or honeycomb. In the analysis of the sandwich construction, it is routinely assumed that the face sheets carry the in-plane and bending loadings and the core transmits the transverse normal and shear loads [Plantema 1966; Vinson 1999]. These classical theories also consider the transverse displacement of the core to be the same as the displacements of the middle surface of the two face sheets. The variation in thickness (compressibility) of the core is often neglected.

However, recent studies show that the core could experience significant changes in thickness [Liang et al. 2007; Nemat-Nasser et al. 2007; Li et al. 2008]. As a consequence, there is an increasing concern on the influence of core compressibility on the behavior of sandwich structures. Efforts to address this issue are demonstrated through the formulation of various advanced high-order sandwich models in the literature [Frostig et al. 1992; Pai and Palazotto 2001; Hohe and Librescu 2003; Li and Kardomateas 2008]. Models considering the core compressibility may not only give a more accurate solution to simpler problems, but may also help to analytically address some otherwise difficult problems such as debond behavior [Li et al. 2001], shock wave propagation and energy absorption in sandwich structures.

In previous work, we derived a high-order sandwich plate theory [Li and Kardomateas 2008], in which the transverse displacement of the core is no longer assumed a constant, but it is a fourth order function

Keywords: composite sandwich shells, compressibility, high-order theory, external pressure.

of the transverse coordinate. The in-plane displacements vary as fifth order functions of the transverse coordinate. The current paper presents an adaptation of this nonlinear high-order core model to the configuration of cylindrical sandwich shells. The derivation procedure of this theory is similar to the one in [Li and Kardomateas 2008] but accommodated to the specific geometry of cylindrical sandwich shells. In the development of the advanced cylindrical sandwich shell model, the following assumptions have been made:

(1) The face sheets satisfy the Kirchhoff–Love assumptions and their thicknesses are small compared with the overall thickness of the sandwich section. The transverse displacements in the faces do not vary through the thickness. In the current paper, the two face sheets are considered to have identical thickness.

(2) The core is compressible in the transverse direction, that is, its thickness may change.

(3) The bonding between the face sheets and the core is assumed perfect.

The paper is organized as follows: We first extend the high-order sandwich plate compressible core theory to the cylindrical sandwich shell. In the derivation, the cylindrical coordinate system (x, s, z) is introduced and located at the middle plane of the core or the face sheets. The transverse displacement of the initial mid-plane is considered as an unknown function of the coordinates (x, s). The axial, circumferencial and transverse displacements in the core are then expressed as functions in terms of the displacements of the two face sheets and the displacement of the core initial mid-plane. The displacement continuity conditions along the interface between the face sheet and the core are employed. We then formulate the governing equations, boundary conditions, and solution procedure for cylindrical sandwich shells. As a representative, the equations for an orthotropic sandwich shell are studied in detail. Next, the numerical results for a typical cylindrical sandwich shell with three orthotropic phases (two face sheets and a core) are presented. Finally, we draw some conclusions and suggestions on future work.

2. Extension of high-order sandwich plate theory to shells

Let a coordinate system (x, s, z) be located at the middle plane of the face sheets or the core with x in the axial direction, s in the circumferential direction, and z in the outward normal direction (Figure 1), and $(u,\ v,\ w)$ be the corresponding displacements. R_i and R_o are the radii of the middle surface of the inner and outer face, respectively; L is the shell length; the outer and inner faces are assumed to have an identical thickness, h_f, and the core thickness is h_c. Also set $R = (R_o + R_i)/2$.

2A. ***Displacement field representation.*** In the classical sandwich model, the compressibility of the core in the thickness direction is ignored. This may give a good approximation in simple and preliminary studies. However, in many more demanding cases, such as a sandwich structure subject to blast/impact loading, consideration of the transverse compressibility of the core may be needed. In the high-order core theory proposed in [Li and Kardomateas 2008], the transverse displacement in the core ($-h_c/2 \le z \le h_c/2$) is in the form

$$w^c(x, s, z) = \left(1 - \frac{2z^2}{h_c^2} - \frac{8z^4}{h_c^4}\right) w_0^c(x, s) + \left(\frac{2z^2}{h_c^2} + \frac{8z^4}{h_c^4}\right) w(x, s) - \left(\frac{z}{h_c} + \frac{4z^3}{h_c^3}\right) \bar{w}(x, s), \tag{1}$$

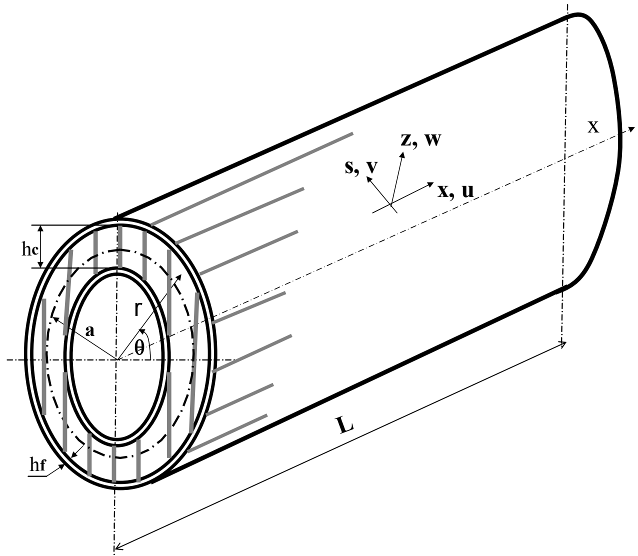

Figure 1. A cylindrical sandwich shell.

and the in-plane displacements in the core are in the form

$$\begin{aligned} u^c(x,s,z) &= u(x,s) - \frac{z}{h_c/2}\bar{u}(x,s) + z\frac{h_f}{h_c} w^c_{,x}(x,s,z), \\ v^c(x,s,z) &= v(x,s) - \frac{z}{h_c/2}\bar{v}(x,s) + z\frac{h_f}{h_c} w^c_{,y}(x,s,z), \end{aligned} \tag{2}$$

In these equations, $w_0^c(x,s)$ is the transverse displacement of the middle surface of the core; $w(x,s)$ is the average of the displacements of top face sheet, $w^t(x,s)$ and bottom face sheet, $w^b(x,s)$; and $\bar{w}(x,s)$ is half of the difference of these displacements. Similar definitions hold for the corresponding in-plane displacements.

This high-order core theory could be extended to other geometric configurations such as shapes with curvature, provided the thickness of the face sheets is small compared to the total thickness of the sandwich structure. In this work, it will be extended to cylindrical sandwich shells with orthotropic phases. The thin face sheets of the shell satisfy the Kirchhoff–Love assumptions. Therefore, setting $h = (h_c + h_f)/2$, one has for the *displacements in the outer face*, $-(h_c/2 + h_f) \le z \le -h_c/2$, the expressions

$$\begin{aligned} u^t(x,s,z) &= u_0^t(x,s) - (z+h)w^t_{,x}(x,s), \\ v^t(x,s,z) &= v_0^t(x,s) - (z+h)w^t_{,s}(x,s), \\ w^t(x,s,z) &= w^t(x,s), \end{aligned} \tag{3}$$

and for the *and displacements in the inner face*, $h_c/2 \le z \le h_c/2 + h_f$,

$$\begin{aligned} u^b(x,s,z) &= u_0^b(x,s) - (z-h)w^b_{,x}(x,s), \\ v^b(x,s,z) &= v_0^b(x,s) - (z-h)w^b_{,s}(x,s), \\ w^b(x,s,z) &= w^b(x,s). \end{aligned} \tag{4}$$

In order to take the core compressibility into account, nonlinear models can be proposed. The one proposed here satisfies all the displacement continuity conditions along the interface between the core and the face sheets, as shown in [Li and Kardomateas 2008].

2B. ***Strain-displacement relation.*** For thin face sheets, one can obtain the strain tensor at a point in the outer face sheet of the cylindric sandwich shell as

$$[\epsilon^t] = \begin{pmatrix} \epsilon_x^t \\ \epsilon_s^t \\ \gamma_{xs}^t \end{pmatrix} = \begin{pmatrix} \epsilon_{0x}^t \\ \epsilon_{0s}^t \\ \gamma_{0xs}^t \end{pmatrix} + (z+h)[\kappa^t] = \begin{pmatrix} u_{0,x}^t \\ v_{0,s}^t + w^t/R_o \\ u_{0,s}^t + v_{0,x}^t \end{pmatrix} + (z+h)[\kappa^t]. \tag{5}$$

A similar expression holds for the strain tensor in the inner face,

$$[\epsilon^b] = \begin{pmatrix} \epsilon_x^b \\ \epsilon_s^b \\ \gamma_{xs}^b \end{pmatrix} = \begin{pmatrix} \epsilon_{0x}^b \\ \epsilon_{0s}^b \\ \gamma_{0xs}^b \end{pmatrix} + (z-h)[\kappa^b] = \begin{pmatrix} u_{0,x}^b \\ v_{0,s}^b + w^b/R_i \\ u_{0,s}^b + v_{0,x}^b \end{pmatrix} + (z-h)[\kappa^b]. \tag{6}$$

In these equations,

$$[\kappa^{t,b}] = \begin{pmatrix} \kappa_x^{t,b} \\ \kappa_s^{t,b} \\ \kappa_{xs}^{t,b} \end{pmatrix} = \begin{pmatrix} -w_{,xx}^{t,b} \\ -w_{,ss}^{t,b} \\ -2w_{,xs}^{t,b} \end{pmatrix}. \tag{7}$$

The core is considered undergoing large rotation with small displacements and its in-plane strains could be neglected. Therefore, one can derive the strain-displacement relations of the core from equations (1) and (2) as follows:

$$\begin{aligned}
\epsilon_z^c &= \left(-\frac{1}{2h_c}+\frac{2z}{h_c^2}-\frac{6z^2}{h_c^3}+\frac{16z^3}{h_c^4}\right)w^t(x,s)-\left(\frac{4z}{h_c^2}+\frac{32z^3}{h_c^4}\right)w_0^c(x,s)+\left(\frac{1}{2h_c}+\frac{2z}{h_c^2}+\frac{6z^2}{h_c^3}+\frac{16z^3}{h_c^4}\right)w^b(x,s),\\
\gamma_{xz}^c &= -\frac{2}{h_c}\bar{u}(x,s)+\eta_1(z)w_{,x}^t(x,s)+\eta_2(z)w_{0,x}^c(x,s)+\eta_3(z)w_{,x}^b(x,s),\\
\gamma_{sz}^c &= -\frac{2}{h_c}\bar{v}(x,s)+\eta_1(z)w_{,s}^t(x,s)+\eta_2(z)w_{0,s}^c(x,s)+\eta_3(z)w_{,s}^b(x,s)-\frac{v^c}{r},
\end{aligned} \tag{8}$$

in which $R-h_c/2 \le r \le R+h_c/2$ and

$$\begin{aligned}
\eta_1(z) &= -\left(\frac{1}{2}+\frac{h_f}{h_c}\right)\frac{z}{h_c}+\left(1+3\frac{h_f}{h_c}\right)\frac{z^2}{h_c^2}-2\left(1+4\frac{h_f}{h_c}\right)\frac{z^3}{h_c^3}+4\left(1+5\frac{h_f}{h_c}\right)\frac{z^4}{h_c^4},\\
\eta_2(z) &= \left(1+\frac{h_f}{h_c}\right)-2\left(1+\frac{3h_f}{h_c}\right)\frac{z^2}{h_c^2}-8\left(1+\frac{5h_f}{h_c}\right)\frac{z^4}{h_c^4},\\
\eta_3(z) &= \left(\frac{1}{2}+\frac{h_f}{h_c}\right)\frac{z}{h_c}+\left(1+3\frac{h_f}{h_c}\right)\frac{z^2}{h_c^2}+2\left(1+4\frac{h_f}{h_c}\right)\frac{z^3}{h_c^3}+4\left(1+5\frac{h_f}{h_c}\right)\frac{z^4}{h_c^4}.
\end{aligned} \tag{9}$$

2C. ***Constitutive relation.*** The face sheets of the shell are made of orthotropic laminated composites and the core is also orthotropic. The stress-strain relationship for any layer of the faces reads as

$$\begin{pmatrix} \sigma_x \\ \sigma_s \\ \tau_{xs} \end{pmatrix} = \begin{pmatrix} Q_{11} & Q_{12} & Q_{16} \\ Q_{12} & Q_{22} & Q_{26} \\ Q_{16} & Q_{26} & Q_{66} \end{pmatrix} \begin{pmatrix} \epsilon_x \\ \epsilon_s \\ \gamma_{xs} \end{pmatrix}, \quad \text{or} \quad [\sigma] = [Q][\epsilon], \tag{10}$$

where the Q_{ij}, for $i, j = 1, 2, 6$, are the reduced stiffness coefficients. The stress-strain relations for the orthotropic core are written as

$$\sigma_z^c = E^c \epsilon_z^c, \quad \tau_{xz} = G_{xz}^c \gamma_{xz}^c, \quad \tau_{sz}^c = G_{sz}^c \gamma_{sz}^c. \tag{11}$$

Here, we define the resultants for the outer face sheet of the sandwich shell by

$$\begin{aligned} [N^t] &= \begin{pmatrix} N_x^t \\ N_s^t \\ N_{xs}^t \end{pmatrix} = \int_{-(h_c/2+h_f)}^{-h_c/2} [\sigma^t]\, dz = \int_{-(h_c/2+h_f)}^{-h_c/2} [Q^t][\epsilon^t]\, dz = [A][\epsilon_0^t] + [B][\kappa^t], \\ [M^t] &= \begin{pmatrix} M_x^t \\ M_s^t \\ M_{xs}^t \end{pmatrix} = \int_{-(h_c/2+h_f)}^{-h_c/2} [\sigma^t] z\, dz = [B][\epsilon_0^t] + [D][\kappa^t], \end{aligned} \tag{12}$$

in which the stiffness coefficients are defined as

$$[\hat{A}_{ij}^t, \hat{B}_{ij}^t, \hat{D}_{ij}^t] = \int_{-(h_c/2+h_f)}^{-h_c/2} Q_{ij}^t [1, (z+h), (z+h)^2] dz. \tag{13}$$

Applying a similar procedure, one can obtain the expressions for the resultants in the inner face sheet.

3. Equilibrium equations and boundary conditions

The cylindrical sandwich shell is assumed subject to external and internal pressure $q^{t,b}(x, s)$. Let U denote the strain energy and W the work of external forces. The variational principle (equivalent to a virtual displacement approach) states that

$$\delta(U - W) = 0, \tag{14}$$

in which

$$\begin{aligned} \delta U = \int_0^L \oint \bigg(& \int_{-h_c/2-h_f}^{-h_c/2} (\sigma_x^t \delta\epsilon_x^t + \sigma_s^t \delta\epsilon_s^t + \tau_{xs}^t \delta\gamma_{xs}^t)(R_o + z)\, dz \\ & + \int_{-h_c/2}^{h_c/2} (\sigma_z^c \delta\epsilon_z^c + \tau_{xz}^c \delta\gamma_{xz}^c + \tau_{sz}^c \delta\gamma_{sz}^c)(R + z)\, dz \\ & + \int_{h_c/2}^{h_c/2+h_f} (\sigma_x^b \delta\epsilon_x^b + \sigma_s^b \delta\epsilon_s^b + \tau_{xs}^b \delta\gamma_{xs}^b)(R_i + z)\, dz \bigg) d\theta\, dx, \\ \delta W = \int_0^L \oint & q^{t,b}(x, s) \delta w^{t,b}\, ds dx + \int_0^L \oint N_x(x, s) \delta u\, ds\, dx. \end{aligned} \tag{15}$$

We now introduce the notation

$$\alpha = \frac{h_f}{h_c} \quad \text{and} \quad \beta = \frac{h_c}{R}.$$

For the thin face sheets of $R_i + z \cong R_i$, $R_o + z \cong R_o$ and $\beta \ll 1$, one can obtain the equilibrium equations and boundary conditions by substituting the stress strain relations (10)–(11) strain-displacement relations (5)–(9) and the displacement representation equations (1)–(4) into (15), then into (14) and employing integration by parts. For the outer face sheet this results in the governing equations

$$\delta u_0^t: \ -N_{x,x}^t - \frac{1}{R_o} N_{x\theta,\theta}^t + G_{xz}^c \left(\frac{4}{\beta}(u_0^t - u_0^b) - \frac{\zeta_1}{\beta} R\, w_{,x}^t - \frac{22}{15} R\, w_{o,x}^c - \frac{\bar{\zeta}_1}{\beta} R\, w_{,x}^b \right) = 0,$$

$$\delta v_0^t: \ -N_{x\theta,x}^t - \frac{1}{R_o} N_{\theta,\theta}^t + G_{sz}^c \left(\zeta_6 v_0^t - \zeta_7 v_0^b + \zeta_8 w_{,\theta}^t + \zeta_9 w_{0,\theta}^c + \zeta_{10} w_{,\theta}^b \right) = 0,$$

$$\begin{aligned} \delta w_0^t: \ -\left(M_{x,xx}^t + \frac{2}{R_o} M_{x\theta,x\theta}^t + \frac{1}{R_o^2} M_{\theta,\theta\theta}^t - \frac{1}{R_o} N_x^t \right) + E_z^c \left(\frac{61+23\beta}{21\beta} w^t + \frac{358+115\beta}{105\beta} w_0^c + \frac{53}{105\beta} w^b \right) \\ + \zeta_1 R G_{xz}^c (u_{0,x}^t - u_{0,x}^b) + G_{sz}^c (\zeta_{11}^t v_{0,\theta}^t - \bar{\zeta}_{11}^t v_{0,\theta}^b) - \zeta_2 R^2 G_{xz}^c w_{,xx}^t - \zeta_{12}^t G_{sz}^c w_{,\theta\theta}^t \\ - \zeta_3 R^2 G_{xz}^c w_{0,xx}^c - \zeta_{13}^t G_{sz}^c w_{0,\theta\theta}^c - \zeta_4 R^2 G_{xz}^c w_{,xx}^b - \zeta_{14}^t G_{sz}^c w_{,\theta\theta}^b - Q_o(x, \theta, t) = 0. \end{aligned}$$

For the compressive core:

$$\begin{aligned} \delta w_0^c: \ E_z^c \left(\frac{358+115\beta}{105\beta} w^t + \frac{716}{105\beta} w_0^c + \frac{358-115\beta}{105\beta} w^b \right) \\ + \tfrac{22}{15} G_{xz}^c (u_{0,x}^t - u_{0,x}^b) + G_{sz}^c (\zeta_{11}^c v_{0,\theta}^t - \bar{\zeta}_{11}^c v_{0,\theta}^b) - \zeta_3 R^2 G_{xz}^c w_{,xx}^t - \zeta_{12}^c G_{sz}^c w_{,\theta\theta}^t \\ - \zeta_5 R^2 G_{xz}^c w_{0,xx}^c - \zeta_{13}^c G_{sz}^c w_{0,\theta\theta}^c - \bar{\zeta}_3 R^2 G_{xz}^c w_{,xx}^b - \zeta_{14}^c G_{sz}^c w_{,\theta\theta}^b = 0. \end{aligned}$$

For the inner face sheet:

$$\delta u_0^b: \ -N_{x,x}^b - \frac{1}{R_i} N_{\theta,\theta}^b - G_{xz}^c \left(\frac{4}{\beta}(u_0^t - u_0^b) - \frac{\zeta_1}{\beta} R\, w_{,x}^t - \frac{22}{15} R\, w_{0,x}^c - \frac{\bar{\zeta}_1}{\beta} R\, w_{,x}^b \right) = 0,$$

$$\delta v_0^b: \ -N_{x\theta,x}^b - \frac{1}{R_i} N_{\theta,\theta}^b - G_{sz}^c \left(\zeta_7 v_0^t - \bar{\zeta}_6 v_0^b - \bar{\zeta}_8 w_{,\theta}^t - \bar{\zeta}_9 w_{0,\theta}^c - \bar{\zeta}_{10} w_{,\theta}^b \right) = 0,$$

$$\begin{aligned} \delta w_0^b: \ -\left(M_{x,xx}^b + \frac{2}{R_i} M_{x\theta,x\theta}^b + \frac{1}{R_i^2} M_{\theta,\theta\theta}^b - \frac{1}{R_i} N_x^b \right) + E_z^c \left(\frac{53}{105\beta} w^t + \frac{358-115\beta}{105\beta} w_0^c + \frac{61-23\beta}{21\beta} w^b \right) \\ + \bar{\zeta}_1 R G_{xz}^c (u_{0,x}^t - u_{0,x}^b) + G_{sz}^c (\zeta_{11}^b v_{0,\theta}^t - \bar{\zeta}_{11}^b v_{0,\theta}^b) - \zeta_4 R^2 G_{xz}^c w_{,xx}^t - \zeta_{12}^b G_{sz}^c w_{,\theta\theta}^t \\ - \bar{\zeta}_3 R^2 G_{xz}^c w_{0,xx}^c - \zeta_{13}^b G_{sz}^c w_{0,\theta\theta}^c - \bar{\zeta}_2 R^2 G_{xz}^c w_{,xx}^b - \zeta_{14}^b G_{sz}^c w_{,\theta\theta}^b - Q_i(x, \theta, t) = 0. \end{aligned}$$

The constants ζ_i and $\zeta_i^{t,c,b}$, for $i = 1, 2, \ldots, 14$, in these equations are functions of β and α and are listed in the Appendix.

The corresponding boundary conditions at $x = 0$, L are

$$
\begin{aligned}
&u_0^t = \widetilde{u}^t \quad \text{or} \quad N_x^t = \widetilde{N}_x^t,\\
&w^t = \widetilde{w}^t \quad \text{or}\\
&\qquad N_x^t w_{,x}^t + M_{x,x}^t + N_{x\theta}^t w_{,y}^t + 2M_{x\theta,x}^t + G_{xz}^c(\zeta_1 R(u_0^b - u_0^t) + \zeta_2 R^2 w_{,x}^t + \zeta_2 R^2 w_{0,x}^c + \zeta_4 R^2 w_{,x}^b) = \widetilde{Q}_x^t,\\
&w_{,x}^t = \widetilde{w}_{,x}^t \quad \text{or} \quad M_x^t = \widetilde{M}_x^t,\\
&w_0^c = \widetilde{w}_0^c \quad \text{or} \quad \tfrac{22}{15} R(u_0^b - u_0^t) + \zeta_3 R^2 w_{,x}^t + \zeta_5 R^2 w_{0,x}^c + \bar{\zeta}_3 R^2 w_{,x}^b = \widetilde{Q}_c,\\
&u_0^b = \widetilde{u}^b \quad \text{or} \quad N_x^b = \widetilde{N}_x^b,\\
&w^b = \widetilde{w}^b \quad \text{or}\\
&\qquad N_x^b w_{,x}^b + M_{x,x}^b + N_{xy}^b w_{,y}^b + 2M_{x\theta,x}^b + G_{xz}^c(\bar{\zeta}_1 R(u_0^b - u_0^t) + \zeta_4 R^2 w_{,x}^t + \bar{\zeta}_3 R^2 w_{0,x}^c + \bar{\zeta}_2 R^2 w_{,x}^b) = \widetilde{Q}_x^t,\\
&w_{,x}^b = \widetilde{w}_{,x}^b \quad \text{or} \quad M_x^b = \widetilde{M}_x^b,
\end{aligned}
$$

where the superscript $\sim$ denotes the known external boundary values. At $\theta = 0$ and 2π, continuity conditions hold.

For the sandwich shell made out of orthotropic materials, the governing equations for the outer face sheet can be rewritten as

$$
\left(A_{11}^t \frac{\partial^2}{\partial x^2} + \frac{A_{66}^t}{R_o^2}\frac{\partial^2}{\partial \theta^2} - \frac{4G_{xz}^c}{\beta}\right)u_0^t + \frac{A_{12}^t + A_{66}^t}{R_o}\frac{\partial^2 v_0^t}{\partial x \partial \theta} + \left(\frac{\zeta_1}{\beta} R G_{xz}^c + \frac{A_{12}^t}{R_o}\right) w_{,x}^t
+ \frac{22}{15} R G_{xz}^c w_{0,x}^c + \frac{4G_{xz}^c}{\beta} u_0^b + \frac{\bar{\zeta}_1}{\beta} G_{xz}^c R w_{,x}^b = 0, \quad (16)
$$

$$
\frac{A_{21}^t + A_{66}^t}{R_o}\frac{\partial^2 u_0^t}{\partial x \partial \theta} + \left(A_{66}^t \frac{\partial^2}{\partial x^2} + \frac{A_{22}^t}{R_o^2}\frac{\partial^2}{\partial \theta^2} - \zeta_6 G_{sz}^c\right) v_0^t + \left(\frac{A_{22}^t}{R_o^2} - \zeta_8 G_{sz}^c\right) w_{,\theta}^t
- \zeta_9 G_{sz}^c w_{0,\theta}^c + \zeta_7 G_{sz}^c v_0^b - \zeta_{10} G_{sz}^c w_{,\theta}^b = 0, \quad (17)
$$

$$
\begin{aligned}
&\left(D_{11}^t \frac{\partial^4}{\partial x^4} + 2\frac{D_{12}^t + 2D_{66}^t}{R_o^2}\frac{\partial^4}{\partial x^2 \theta^2} + \frac{D_{22}^t}{R_o^4}\frac{\partial^4}{\partial \theta^4} + \frac{(61+23\beta)E_z^c}{21\beta} - \zeta_2 R^2 G_{xz}^c \frac{\partial^2}{\partial x^2} - \zeta_{12}^t G_{sz}^c \frac{\partial^2}{\partial \theta^2} + \frac{A_{12}^t}{R_o^2}\right) w^t\\
&\quad + \frac{A_{11}^t}{R_o}\frac{\partial u_0^t}{\partial x} + \zeta_1 R G_{xz}^c \frac{\partial}{\partial x}(u_0^t - u_0^b) + \left(\frac{(358+115\beta)E_z^c}{105\beta} - \zeta_3 R^2 G_{xz}^c \frac{\partial^2}{\partial x^2} - \zeta_{13}^t G_{sz}^c \frac{\partial^2}{\partial \theta^2}\right) w_0^c\\
&\quad + \frac{A_{12}^t}{R_o^2}\frac{\partial v_0^t}{\partial \theta} + G_{sz}^c \frac{\partial}{\partial \theta}(\zeta_{11}^t v_0^t - \bar{\zeta}_{11}^t v_0^b) + \left(\frac{53E_z^c}{105\beta} - \zeta_4 R^2 G_{xz}^c \frac{\partial^2}{\partial x^2} - \zeta_{14}^t G_{sz}^c \frac{\partial^2}{\partial \theta^2}\right) w^b = Q_o(x,\theta). \quad (18)
\end{aligned}
$$

Similarly, the equation for the core can be recast as

$$
\begin{aligned}
&\frac{22}{15} G_{xz}^c u_{0,x}^t + G_{sz}^c \zeta_{11}^c v_{0,\theta}^t + \left(\frac{(358+115\beta)E_z^c}{105\beta} - \zeta_3 R^2 G_{xz}^c \frac{\partial^2}{\partial x^2} - \zeta_{12}^c G_{sz}^c \frac{\partial^2}{\partial \theta^2}\right) w^t\\
&\quad + \left(\frac{716E_z^c}{105\beta} - \zeta_5 R^2 G_{xz}^c \frac{\partial^2}{\partial x^2} - \zeta_{13}^c G_{sz}^c \frac{\partial^2}{\partial \theta^2}\right) w_0^c - \frac{22}{15} G_{xz}^c u_{0,x}^b - \bar{\zeta}_{11}^c G_{sz}^c v_{0,\theta}^b\\
&\quad + \left(\frac{(358-115\beta)E_z^c}{105\beta} - \bar{\zeta}_3 R^2 G_{xz}^c \frac{\partial^2}{\partial x^2} - \zeta_{14}^c G_{sz}^c \frac{\partial^2}{\partial \theta^2}\right) w^b = 0. \quad (19)
\end{aligned}
$$

Finally, for the inner face sheet:

$$\left(A_{11}^{b}\frac{\partial^2}{\partial x^2}+\frac{\hat{A}_{66}^{b}}{R_i^2}\frac{\partial^2}{\partial\theta^2}-\frac{4G_{xz}^{c}}{\beta}\right)u_0^{b}+\frac{A_{12}^{b}+A_{66}^{b}}{R_i}\frac{\partial^2 v_0^{b}}{\partial x\partial\theta}+\left(\frac{\bar{\zeta}_1}{\beta}RG_{xz}^{c}+\frac{A_{12}^{b}}{R_i}\right)w_{,x}^{b}$$
$$+\frac{22}{15}RG_{xz}^{c}w_{0,x}^{c}+\frac{4G_{xz}^{c}}{\beta}u_0^{t}+G_{xz}^{c}\frac{\zeta_1}{\beta}Rw_{,x}^{t}=0, \quad (20)$$

$$\frac{A_{21}^{b}+A_{66}^{b}}{R_i}\frac{\partial^2 u_0^{b}}{\partial x\partial\theta}+\left(A_{66}^{b}\frac{\partial^2}{\partial x^2}+\frac{A_{22}^{b}}{R_i^2}\frac{\partial^2}{\partial\theta^2}-\bar{\zeta}_6G_{sz}^{c}\right)v_0^{b}-\left(\bar{\beta}_{10}G_{sz}^{c}-\frac{A_{22}^{b}}{R_i^2}\right)w_{,\theta}^{b}$$
$$-\bar{\zeta}_9G_{sz}^{c}w_{0,\theta}^{c}+\zeta_7G_{sz}^{c}v_0^{t}-\bar{\zeta}_8G_{sz}^{c}w_{,\theta}^{t}=0, \quad (21)$$

$$\left[D_{11}^{b}\frac{\partial^4}{\partial x^4}+2\frac{D_{12}^{b}+2D_{66}^{b}}{R_i^2}\frac{\partial^4}{\partial x^2\partial\theta^2}+\frac{D_{22}^{b}}{R_i^4}\frac{\partial^4}{\partial\theta^4}+\frac{(61-23\beta)E_z^{c}}{21\beta}-\left(\bar{\zeta}_2R^2G_{xz}^{c}\frac{\partial^2}{\partial x^2}+\zeta_{14}^{b}G_{sz}^{c}\frac{\partial^2}{\partial\theta^2}\right)+\frac{A_{12}^{b}}{R_i^2}\right]w^{b}$$
$$+\bar{\zeta}_1RG_{xz}^{c}\frac{\partial}{\partial x}(u_0^{t}-u_0^{b})+\frac{A_{11}^{b}}{R_o}\frac{\partial u_0^{b}}{\partial x}+\left(\frac{(358-115\beta)E_z^{c}}{105\beta}-\bar{\beta}_3R^2G_{xz}^{c}\frac{\partial^2}{\partial x^2}-\zeta_{13}^{b}G_{sz}^{c}\frac{\partial^2}{\partial\theta^2}\right)w_0^{c}$$
$$+\frac{A_{12}^{b}}{R_i^2}\frac{\partial v_0^{b}}{\partial\theta}+G_{sz}^{c}\frac{\partial}{\partial\theta}(\zeta_{11}^{b}v_0^{t}-\bar{\zeta}_{11}^{b}v_0^{b})+\left(\frac{53E_z^{c}}{105\beta}-\zeta_4R^2G_{xz}^{c}\frac{\partial^2}{\partial x^2}-\zeta_{12}^{b}G_{sz}^{c}\frac{\partial^2}{\partial\theta^2}\right)w^{t}=Q_i(x,\theta,t). \quad (22)$$

It should be noted that since this new core theory is a three-dimensional approximation model for the core (but more efficient than a complete three-dimensional elasticity approach), none of the existing shell theories could produce identical governing equations.

4. A cylindrical sandwich shell under external pressure

In this section the solution procedure for the response of sandwich shells will be demonstrated through the study of simply supported cylindrical shell under external pressure. The boundary conditions are

$$w^t=0,\quad w^c=0,\quad w^b=0;\qquad M_x^t=0,\quad M_x^b=0,\quad \text{for } x=0,L.$$

and v_0^t, w^t, w^c, v_0^b, w^b, M_{yy}^t and M_{yy}^b are continuous at $\theta=0,2\pi$. As such, the displacements can be set in the form

$$u_0^{t}=\sum_{\substack{m=0\\n=0}}^{M,N}U_{mn}^{t}\cos\frac{m\pi x}{L}\cos n\theta,\quad u_0^{b}=\sum_{\substack{m=0\\n=0}}^{M,N}U_{mn}^{b}\cos\frac{m\pi x}{L}\cos n\theta,$$
$$v_0^{t}=\sum_{\substack{m=0\\n=0}}^{M,N}V_{mn}^{t}\sin\frac{m\pi x}{L}\sin n\theta,\quad v_0^{b}=\sum_{\substack{m=0\\n=0}}^{M,N}V_{mn}^{b}\sin\frac{m\pi x}{L}\sin n\theta, \quad (23)$$
$$w^{t}=\sum_{\substack{m=0\\n=0}}^{M,N}W_{mn}^{t}\sin\frac{m\pi x}{L}\cos n\theta,\quad w^{b}=\sum_{\substack{m=0\\n=0}}^{M,N}W_{mn}^{b}\sin\frac{m\pi x}{L}\cos n\theta,\quad w^{c}=\sum_{\substack{m=0\\n=0}}^{M,N}W_{mn}^{c}\sin\frac{m\pi x}{L}\cos n\theta,$$

where U^t_{mn}, V^t_{mn}, W^t_{mn}, W^c_{mn}, U^b_{mn}, V^b_{mn} and W^b_{mn} are constants to be determined. The applied external and internal loading $Q_o(x,\theta)$ and $Q_i(x,\theta)$ can be, respectively, expressed in the form

$$Q_o(x,\theta)=\sum_{\substack{m=0\\n=0}}^{M,N}\hat{Q}^o_{mn}\sin\frac{m\pi x}{L}\cos n\theta,\qquad Q_i(x,\theta)=\sum_{\substack{m=0\\n=0}}^{M,N}\hat{Q}^i_{mn}\sin\frac{m\pi x}{L}\cos n\theta,\tag{24}$$

where $0\le\theta\le 2\pi$ and the coefficients are defined for $m=0,\dots,M$ and $n=0,\dots,N$ as

$$\hat{Q}^o_{mn}=\frac{2}{a\pi}\int_0^L\int_0^\Theta Q_o(x,\theta)\,dx\,d\theta,\qquad \hat{Q}^i_{mn}=\frac{2}{a\pi}\int_0^L\int_0^\Theta Q_i(x,\theta)\,dx\,d\theta.\tag{25}$$

Substituting equations (23)–(25) into the governing equations (16)–(22), one can obtain a set of equations in matrix form:

$$[K^{MN}]U_{mn}=F_{mn},\tag{26}$$

where the displacement vector U_{mn} is defined as $U_{mn}=[U^t_{mn}, V^t_{mn}, W^t_{mn}, W^c_{mn}, U^b_{mn}, V^b_{mn}, W^b_{mn}]^T$ and the loading vector F_{mn} as $[0.0, 0.0, \hat{Q}^o_{mn}, 0.0, 0.0, 0.0, \hat{Q}^i_{mn}]^T$. The $[K^{MN}]$ is a 7×7 matrix, whose entries are given on the next page. Once the applied loading is given, the displacements can be found by solving (26) for each pair (m,n) until the solutions in form of (23) converge as m and n increase.

Results for a cylindrical sandwich shell under localized external pressure. Assume that a constant pressure loading is applied on a portion of the outer face sheet:

$$p(x,\theta)=p_0,\quad 0\le x\le a,\quad -\frac{\pi}{4}\le\theta\le\frac{\pi}{4}.$$

From equations (24) and (25) one can obtain the following loading in the transformed space for $m=1,2,3,\dots$:

$$Q_{m0}=\frac{2}{m\pi}p_0\sin^2\frac{m\pi}{2},\qquad Q_{mn}=\frac{8}{mn\pi^2}p_0\sin^2\frac{m\pi}{2}\sin\frac{n\pi}{4}\quad n=1,2,3,\dots$$

The relationship for the Poisson's ratio, $\nu_{ij}=\nu_{ji}E_i/E_j$, will be applied since the sandwich structure consists of orthotropic phases. In the following study, we set the radius of the core middle plane, $R=0.8$ m. Its core thickness is $h_c=\beta R$ with $\beta=1/10$. The thickness of two face sheets is the same, $h_f=\alpha h_c$, with $\alpha=1/20$. The length of the sandwich shell is set as $L=1.5$ m. The face sheets of this cylindrical sandwich shell have the following elastic constants (in GPa): $E^f_1=40.0$, $E^f_2=10.0$, $E^f_3=10.0$, $G^f_{12}=4.50$, $G^f_{23}=3.50$, $G^f_{31}=4.50$; Poisson's ratios: $\nu^f_{12}=0.065$, $\nu^f_{31}=0.26$, $\nu^f_{23}=0.40$. The core is made of orthotropic honeycomb material with elastic constants reading as (in GPa): $E^c_1=E^c_2=0.032$, $E^c_3=E^c_z=0.30$, $G^c_{12}=0.013$, $G^c_{31}=0.048$, $G^c_{23}=0.048$; Poisson's ratios: $\nu^c_{12}=\nu^c_{31}=\nu^c_{32}=0.25$.

In the computation of results, $M=16$ and $N=10$ in equations (23) is required for the numerical convergence. The displacements are normalized by $p_0h_{tot}/(E_f)$, where h_{tot} is the total thickness of the shell; the stress normalized by p_0 in the following study. Figure 2 plots the normalized mid-plane displacements in the outer face sheet, core and inner face sheet as a function of x at $\theta=0$. One can readily see that the displacements in the three phases of the cylindrical shell are not identical, implying that the current theory can capture the compressibility of the core in the cylindrical sandwich shells. It can also be seen that the displacement difference in magnitude between the outer face and the core mid-plane is

11 $-\hat{A}^t_{11}\left(\frac{m\pi}{a}\right)^2-\hat{A}^t_{66}\left(\frac{n}{R_o}\right)^2-G^c_{xz}/\alpha$ 12 $-(\hat{A}^t_{12}+\hat{A}^t_{66})\frac{m\pi}{a}\frac{n}{R_o}$ 13 $-(\hat{A}^t_{12}/R_o+\beta_0 RG^c_{xz})\frac{m\pi}{a}$

14 $-\frac{11}{15}G^c_{xz}\frac{m\pi}{a}$ 15 G^c_{xz}/α 16 0 17 $-\beta_1 G^c_{xz}R\frac{m\pi}{a}$ 21 $-(\hat{A}^t_{21}+\hat{A}^t_{66})\frac{m\pi}{a}\frac{n}{R_o}$

22 $-\hat{A}^t_{66}\left(\frac{m\pi}{a}\right)^2-\hat{A}^t_{22}\left(\frac{n}{R_o}\right)^2+\beta_2 G^c_{sz}$ 23 $(\hat{A}^t_{22}/R^2_o+\frac{2+\alpha}{2-\alpha}\beta_4 G^c_{sz})n$ 24 $(2+\alpha)\beta_5 G^c_{sz}n$

25 0 26 $-\beta_3 G^c_{sz}$ 27 $\beta_4 G^c_{sz}n$ 31 $-R\beta_6 G^c_{xz}\frac{m\pi}{a}$ 32 $\beta_4\frac{2+\alpha}{2-\alpha}G^c_{sz}n$

33 $\hat{D}^t_{111}\left(\frac{m\pi}{a}\right)^4+2\frac{\hat{D}^t_{112}+2\hat{D}^t_{166}}{R^2_o}\left(\frac{m\pi}{a}\right)^2 n^2+\frac{\hat{D}^t_{122}}{R^4_o}n^4+\frac{(61-23\alpha)E^c_z}{21\alpha}+\beta_7 G^c_{xz}\left(\frac{m\pi}{a}\right)^2+\beta_8 G^c_{sz}n^2$

34 $\hat{D}^t_{211}\left(\frac{m\pi}{a}\right)^4+2\frac{\hat{D}^t_{212}+2\hat{D}^t_{266}}{R^2_o}\left(\frac{m\pi}{a}\right)^2 n^2+\frac{\hat{D}^t_{222}}{R^4_o}n^4-\frac{(358-115\alpha)E^c_z}{105\alpha}+\left(\beta_9 G^c_{xz}\frac{m\pi}{a}\right)^2+\beta_{10}G^c_{sz}n^2$

35 $R\beta_6 G^c_{xz}\frac{m\pi}{a}$ 36 $-\beta_4\frac{2+\alpha}{2-\alpha}G^c_{sz}n$

37 $\hat{D}^t_{311}\left(\frac{m\pi}{a}\right)^4+2\frac{\hat{D}^t_{312}+2\hat{D}^t_{366}}{R^2_o}\left(\frac{m\pi}{a}\right)^2 n^2+\frac{\hat{D}^t_{322}}{R^4_o}n^4+\frac{53E^c_z}{105}-\beta_{11}G^c_{xz}\left(\frac{m\pi}{a}\right)^2-\beta_{12}G^c_{sz}n^2$

41 $-\frac{11}{15}G^c_{xz}\frac{m\pi}{a}$ 42 $-G^c_{sz}(2+\alpha)\beta_5 n$ 43 $-\left(\frac{(358-115\alpha)E^c_z}{105\alpha}-\beta_9 G^c_{xz}\left(\frac{m\pi}{a}\right)^2-\beta_{10}G^c_{sz}n^2\right)$

44 $\frac{716E^c_z}{105\alpha}+\beta_{13}G^c_{xz}\left(\frac{m\pi}{a}\right)^2-\beta_{14}G^c_{sz}n^2$ 45 $\frac{11}{15}G^c_{xz}\frac{m\pi}{a}$ 46 $(2-\alpha)G^c_{sz}\beta_5 n$

47 $-\frac{(358+115\alpha)E^c_z}{105\alpha}-\beta_{15}G^c_{xz}\left(\frac{m\pi}{a}\right)^2-\beta_{16}G^c_{sz}n^2$ 51 G^c_{xz}/α 52 0 53 $\beta_0 G^c_{xz}R\frac{m\pi}{a}$

54 $\frac{11}{15}G^c_{xz}\frac{m\pi}{a}$ 55 $-\hat{A}^b_{11}\left(\frac{m\pi}{a}\right)^2-\hat{A}^b_{66}\left(\frac{n}{R_i}\right)^2-G^c_{xz}/\alpha$ 56 $-(\hat{A}^b_{12}+\hat{A}^b_{56})\frac{m\pi}{a}\frac{n}{R_i}$

57 $(\beta_1 RG^c_{xz})\frac{m\pi}{a}-\hat{A}^b_{12}/R_o$ 61 0 62 $-\beta_3 G^c_{sz}n$ 63 $\beta_4 G^c_{sz}n$ 64 $(2-\alpha)\beta_5 G^c_{sz}n$

65 $-(\hat{A}^t_{21}+\hat{A}^t_{66})\frac{m\pi}{a}\frac{n}{R_i}$ 66 $\hat{A}^b_{66}\left(\frac{m\pi}{a}\right)^2+\hat{A}^b_{22}\left(\frac{n}{R_i}\right)^2+\beta_2 G^c_{sz}$ 67 $\left(\frac{\hat{A}^b_{22}}{R^2_i}-\frac{2-\alpha}{2+\alpha}\beta_4 G^c_{sz}\right)n$

71 $-R\beta_1 G^c_{xz}\frac{m\pi}{a}$ 72 $-\beta_4 G^c_{sz}n$

73 $\hat{D}^b_{111}\left(\frac{m\pi}{a}\right)^4+2\frac{\hat{D}^b_{112}+2\hat{D}^b_{166}}{R^2_i}\left(\frac{m\pi}{a}\right)^2 n^2+\frac{\hat{D}^b_{122}}{R^4_i}n^4+\frac{53E^c_z}{105}-\beta_{11}G^c_{xz}\left(\frac{m\pi}{a}\right)^2-\beta_{12}G^c_{sz}n^2$

74 $\hat{D}^b_{211}\left(\frac{m\pi}{a}\right)^4+2\frac{\hat{D}^b_{212}+2\hat{D}^b_{266}}{R^2_i}\left(\frac{m\pi}{a}\right)^2 n^2+\frac{\hat{D}^b_{222}}{R^4_i}n^4-\frac{(358+115\alpha)E^c_z}{105\alpha}+\beta_{15}G^c_{xz}\left(\frac{m\pi}{a}\right)^2+\beta_{16}G^c_{sz}n^2$

75 $R\beta_1 G^c_{xz}\frac{m\pi}{a}$ 76 $-\beta_4\frac{2-\alpha}{2+\alpha}G^c_{sz}n$

77 $\hat{D}^b_{311}\left(\frac{m\pi}{a}\right)^4+2\frac{\hat{D}^b_{312}+2\hat{D}^b_{366}}{R^2_i}\left(\frac{m\pi}{a}\right)^2 n^2+\frac{\hat{D}^b_{322}}{R^4_i}n^4+\frac{(61+23\alpha)E^c_z}{21\alpha}+\beta_{17}G^c_{xz}\left(\frac{m\pi}{a}\right)^2+\beta_{18}G^c_{sz}n^2$

Table 1. Matrix $[K^{MN}]$ in (26). The number 12 introduces the entry $M=1$, $N=2$, etc.

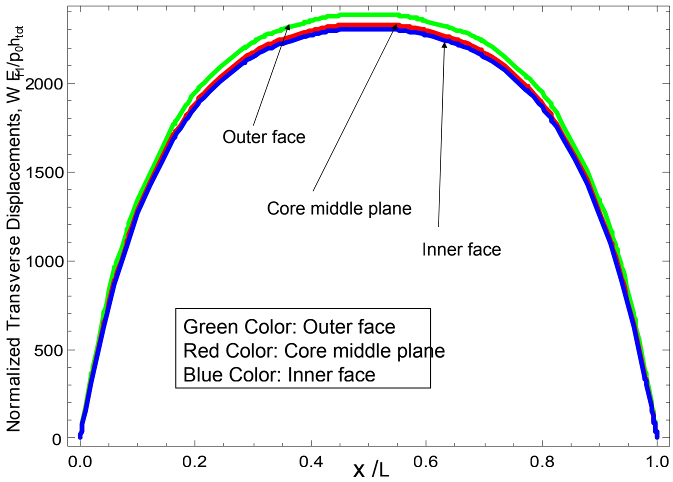

Figure 2. Mid-plane transverse displacement in the outer face sheet, core and inner face sheet as a function of x at $\theta = 0$.

larger than that between the core mid-plane and the inner face sheet. This observation demonstrates that the radial displacement in the core is a nonlinear function with respect to the radial coordinate.

Figure 3 presents the cross-sectional shapes of the outer face sheet mid-plane cut through $x = L/6$, $L/4$ and $L/2$. The undeformed shape is also plotted as a reference. It can be seen that the cross-section deforms the most from its original shape at the middle of the cylindrical shell in the axial direction ($x = L/2$), in particular within the region $-\pi/4 \leq \theta \leq \pi/4$ of each cross section where the loading is applied.

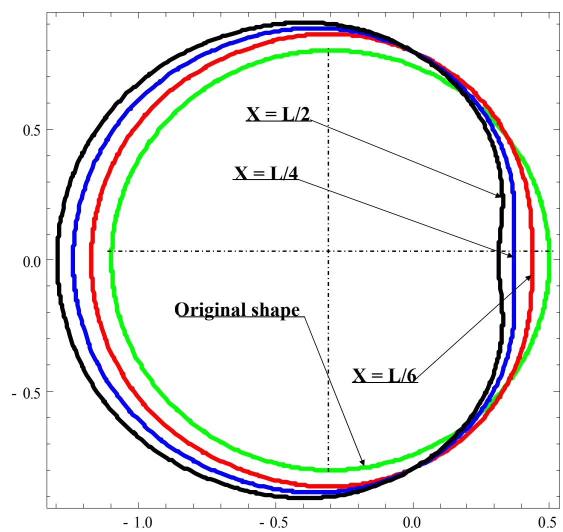

Figure 3. The deformed cross-sectional shape of the mid-plane in the outer face sheet at $x = L/6$, $L/4$ and $L/2$, along with the undeformed cross-sectional shape.

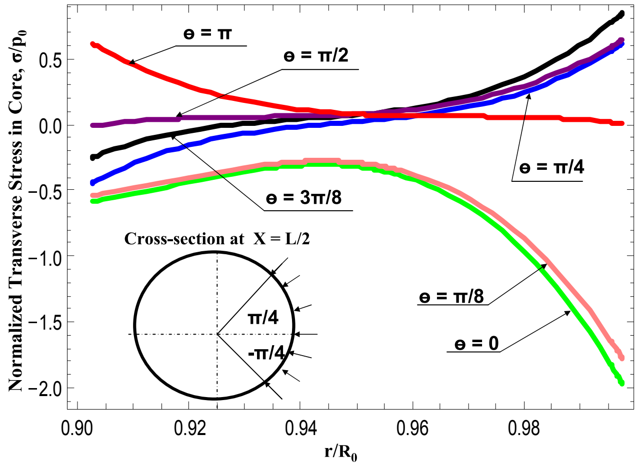

Figure 4. Variation of transverse stress through the core of the shell for various θ.

We also investigated the transverse (radial) stress distribution in the core of the sandwich shell, one of the most interesting issues in sandwich structural studies. The results are plotted in Figures 4 and 5 (where $+$ denotes expansion pressure and $-$ compressive pressure). Figure 4 shows the transverse stress for the cross-section $x = L/2$ at different θ. We see that the stress varies with θ from completely compressive (at $\theta = 0$) to completely expansive pressure (at $\theta = \pi$). The maximum stress in magnitude happens along the interface between the core and the outer face sheet on which the loading is applied. This maximum stress is compressive. The maximum expansion stress happens at $\theta = \pi/2$, also at the interface between the core the outer face sheet. This suggests that these could be the possible positions for damage initiation — useful knowledge for the optimal design of cylindrical sandwich shells.

The variation of the transverse stresses at $\theta = 0$ for different cross-sections is presented in Figure 5. The results show that the maximum compressive stress for each cross-section occurs along the interface

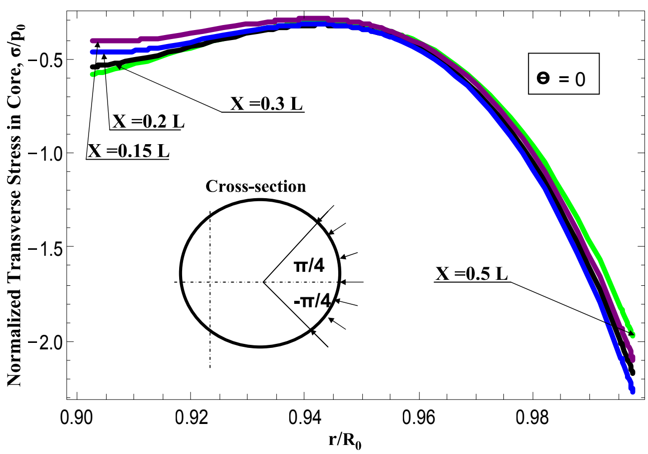

Figure 5. Cross-sectional shape of the mid-plane of the outer face sheet for various x.

between the outer face sheet and the core. Another interesting observation in this study is that the global maximum compressive stress (of 2.2662) is found around ($x = 0.2L, \theta = 0$), not at ($x = 0.5L, \theta = 0$), where the transverse compressive stress is 1.98787. If one uses the value at ($x = 0.5L, \theta = 0$) as the design criterion, it could yield 12% error. This approximation may be acceptable in some preliminary designs. For an accurate design, one may have to find out the exact global maximum compressive and expansion stresses. Therefore, the study in this work can provide useful guidelines for the design of advanced cylindrical sandwich shells.

5. Conclusions

We have developed an analytical solution for a cylindrical sandwich shell with flexible core. A nonlinear high order model for cylindrical sandwich shells is formulated by extending our previous work on sandwich plates. The governing equations and boundary conditions thus derived have the compressibility of the core included. The solution procedure for an orthotropic sandwich cylindrical shell is studied in detail. Numerical results for external pressure loading exerted on a portion of the outer face sheet are presented. The observations from the numerical results suggest the following conclusions:

(1) The mid-plane displacements of the outer face sheet, the core and the inner face sheet are not identical.

(2) The transverse displacement distribution in the core through its thickness is a nonlinear function of the radial coordinate.

(3) The maximum stress in magnitude occurs at the interface between the core and the face sheets on which the loading is applied.

(4) The present nonlinear model is able to capture the nonlinear stress and displacement profiles and predict the global maximum stress and its location. Therefore, this study can have significance for the design of advanced cylindrical sandwich shells.

Acknowledgments

The financial support of the Office of Naval Research, Grant N00014-07-10373, and the interest and encouragement of the Grant Monitor, Dr. Y. D. S. Rajapakse, are gratefully acknowledged.

Appendix: Constants appearing in the governing equations (page 1458)

When constants are given together, separated by commas, the upper signs correspond to the symbol(s) before the comma and the lower signs to the symbol(s) after the comma.

$$\zeta_1, \bar{\zeta}_1 = (8\beta + 30\alpha\beta \pm 4\beta^2 \pm 11\alpha\beta^2)/30,$$

$$\zeta_2, \bar{\zeta}_2 = (116\beta + 746\alpha\beta + 1235\alpha^2\beta \pm 47\beta^2 \pm 315\alpha\beta^2 \pm 517\alpha^2\beta^2)/1260,$$

$$\zeta_3, \bar{\zeta}_3 = (74\beta + 74\alpha\beta - 766\alpha^2\beta \pm 37\beta^2 \mp 286\alpha^2\beta^2)/1260,$$

$$\zeta_4 = (-22\beta - 22\alpha\beta + 161\alpha^2\beta)/1260, \qquad \zeta_5 = (776\beta + 776\alpha\beta + 1532\alpha^2\beta)/1260,$$

$$\zeta_6, \bar{\zeta}_6 = \frac{1}{4\beta^2}\Big[\pm 16\beta^2 + (4 \mp \beta)^2 \log\frac{2+\beta}{2-\beta}\Big], \qquad \zeta_7 = \frac{1}{4\beta^2}\Big[(16 - \beta^2)\log\frac{2+\beta}{2-\beta}\Big],$$

$$\zeta_8, \zeta_{11}^t = \mp\frac{1}{60(2+\beta)\beta^5}\Big[2\beta\big[2(240-60\beta+20\beta^2-5\beta^3-4\beta^4+13\beta^5) + \alpha(9120-1080\beta+220\beta^2+180\beta^3-216\beta^4+137\beta^5)\big] - 15\big[64-16\beta-4\beta^4+\beta^5+2\alpha(608-72\beta-36\beta^2+18\beta^3-23\beta^4+3\beta^5)\big]\log\frac{2+\beta}{2-\beta}\Big],$$

$$\bar{\zeta}_8 = \bar{\zeta}_{11}^t = \frac{1}{60(2+\beta)\beta^5}\Big[2\beta\big[2(240+60\beta+20\beta^2+5\beta^3-4\beta^4+3\beta^5) + \alpha(9120+2520\beta+580\beta^2+300\beta^3-96\beta^4+47\beta^5)\big] + 15(2+\beta)\big[-32+8\beta-4\beta^2+2\beta^3+\beta^4+2\alpha(-304+68\beta-28\beta^2+11\beta^3+3\beta^4)\big]\log\frac{2+\beta}{2-\beta}\Big],$$

$$\zeta_9, \zeta_{11}^c = \pm\frac{1}{30\beta^5}\Big[8\beta\big[60-15\beta+20\beta^2-5\beta^3-11\beta^4+\alpha(720-150\beta+180\beta^2-35\beta^3-11\beta^4)\big] - 15\big[32-8\beta+8\beta^2-2\beta^3-4\beta^4+\beta^5+2\alpha(192-40\beta+32\beta^2-6\beta^3-8\beta^4+\beta^5)\big]\log\frac{2+\beta}{2-\beta}\Big],$$

$$\bar{\zeta}_9 = \bar{\zeta}_{11}^c = \frac{1}{30\beta^5}\Big[8\beta\big[-60-15\beta-20\beta^2-5\beta^3+11\beta^4+\alpha(-720-150\beta-180\beta^2-35\beta^3+11\beta^4)\big] + 15\big[32+8\beta+8\beta^2+2\beta^3-4\beta^4-\beta^5+2\alpha(192+40\beta+32\beta^2+6\beta^3-8\beta^4-\beta^5)\big]\log\frac{2+\beta}{2-\beta}\Big],$$

$$\zeta_{10}, \zeta_{11}^b = \pm\frac{1}{60(2-\beta)\beta^5}\Big[2\beta\big[2(-240+60\beta-20\beta^2+5\beta^3+4\beta^4+3\beta^5) + \alpha(-9120+2520\beta-580\beta^2+300\beta^3+96\beta^4+47\beta^5)\big] + 15\big[64-16\beta-4\beta^4+\beta^5+2\alpha(608-168\beta-12\beta^2-6\beta^3-17\beta^4+3\beta^5)\big]\log\frac{2+\beta}{2-\beta}\Big],$$

$$\bar{\zeta}_{10} = \bar{\zeta}_{11}^b = \frac{-1}{60(2-\beta)\beta^5}\Big[2\beta\big[2(-240-60\beta-20\beta^2-5\beta^3+4\beta^4+13\beta^5) + \alpha(-9120-1080\beta-220\beta^2+180\beta^3+216\beta^4+137\beta^5)\big] + 15(2-\beta)\big[32+24\beta+12\beta^2+6\beta^3+\beta^4+2\alpha(304+188\beta+76\beta^2+29\beta^3+3\beta^4)\big]\log\frac{2+\beta}{2-\beta}\Big],$$

$$\zeta_{12}^t, \zeta_{14}^b = \frac{1}{420(2\pm\beta)^2\beta^8}\Big[4\beta\big[-6720-560\beta^2+756\beta^4+55\beta^6+20\beta^8\pm23\beta^9 + 7\alpha^2(-369600\mp73920\beta+160\beta^2\mp18640\beta^3+17700\beta^4\pm1576\beta^5 - 188\beta^6\pm484\beta^7-97\beta^8\pm91\beta^9) + \alpha(-309120\mp33600\beta-8960\beta^2\mp11200\beta^3+23576\beta^4\pm980\beta^5 + 640\beta^6\pm520\beta^7-30\beta^8\pm243\beta^9)\big] + 105(2\pm\beta)^2\big[(8\mp4\beta+2\beta^2\mp\beta^3)^2+4\alpha(736\mp656\beta+432\beta^2\mp248\beta^3+78\beta^4\mp21\beta^5+4\beta^6) + 4\alpha^2(6160\mp4928\beta+2872\beta^2\mp1432\beta^3+385\beta^4\mp86\beta^5+13\beta^6)\big]\log\frac{2+\beta}{2-\beta}\Big],$$

$$\zeta_{12}^b, \zeta_{14}^t = \frac{-1}{420(4-\beta^2)\beta^8}\Big[4\beta\big[6720+560\beta^2-756\beta^4-55\beta^6+26\beta^8 + 7\alpha^2(369600-4480\beta^2-20220\beta^4-316\beta^6+89\beta^8) + \alpha(309120+8960\beta^2-23576\beta^4-640\beta^6+286\beta^8)\big] - 105(\beta^2-4)\big[(\beta^2-4)(4+\beta^2)^2+8\alpha(-368-72\beta^2+13\beta^4+2\beta^6) + 4\alpha^2(-6160-952\beta^2+127\beta^4+13\beta^6)\big]\log\frac{2+\beta}{2-\beta}\Big],$$

$$\left.\begin{array}{l}\zeta_{12}^c, \zeta_{13}^t \\ \zeta_{13}^b, \zeta_{14}^c\end{array}\right\} = \frac{1}{210(2\pm\beta)\beta^8}\Big[2\beta\big[6720+2240\beta^2-1036\beta^4-174\beta^6+47\beta^8 \\ +\alpha^2(1680000\pm154560\beta+318080\beta^2\pm73360\beta^3-87640\beta^4\pm3192\beta^5 \\ -6624\beta^6\mp684\beta^7+103\beta^8) \\ +\alpha(248640\pm13440\beta+62720\beta^2\pm7840\beta^3-23212\beta^4\mp112\beta^5-2350\beta^6 \\ \mp376\beta^7+235\beta^8)\big] \\ -105\big[(4-\beta^2)^2(8+6\beta^2+\beta^4) \\ +4\alpha^2(8000\pm736\beta+848\beta^2\pm288\beta^3-588\beta^4\mp18\beta^5-11\beta^6\mp7\beta^7+4\beta^8) \\ +\alpha(4736\pm256\beta+800\beta^2\pm128\beta^3-568\beta^4\mp16\beta^5-18\beta^6\mp8\beta^7+9\beta^8)\big]\log\frac{2+\beta}{2-\beta}\Big],$$

$$\zeta_{13}^c = \frac{1}{105\beta^8}\Big[4\beta\big[-1680-980\beta^2+224\beta^4+117\beta^6+14\alpha(-3360-1600\beta^2+208\beta^4+81\beta^6) \\ +\alpha^2(-268800-105560\beta^2+5040\beta^4+1843\beta^6)\big] \\ +105\big[(-8-2\beta^2+\beta^4)^2+4\alpha^2(2560+792\beta^2-146\beta^4-21\beta^6+\beta^8) \\ +4\alpha(448+176\beta^2-48\beta^4-10\beta^6+\beta^8)\big]\log\frac{2+\beta}{2-\beta}\Big],$$

References

[Frostig et al. 1992] Y. Frostig, M. Baruch, O. Vilnay, and I. Sheinman, "High-order theory for sandwich-beam behavior with transversely flexible core", *J. Eng. Mech.* (*ASCE*) **118**:5 (1992), 1026–1043.

[Hohe and Librescu 2003] J. Hohe and L. Librescu, "A nonlinear theory for doubly curved anisotropic sandwich shells with transversely compressible core", *Int. J. Solids Struct.* **40**:5 (2003), 1059–1088.

[Li and Kardomateas 2008] R. Li and G. A. Kardomateas, "Nonlinear high-order core theory for sandwich plates with orthotropic phases", *AIAA J.* **46**:11 (2008), 2926–2934.

[Li et al. 2001] R. Li, Y. Frostig, and G. A. Kardomateas, "Nonlinear high-order response of imperfect sandwich beams with delaminated faces", *AIAA J.* **39**:9 (2001), 1782–1787.

[Li et al. 2008] R. Li, G. A. Kardomateas, and G. J. Simitses, "Nonlinear response of a shallow sandwich shell with compressible core to blast loading", *J. Appl. Mech.* (*ASME*) **75**:6 (2008), #061023.

[Liang et al. 2007] Y. Liang, A. V. Spuskanyuk, S. E. Flores, D. R. Hayhurst, J. W. Hutchinson, R. M. McMeeking, and A. G. Evans, "The response of metallic sandwich panels to water blast", *J. Appl. Mech.* (*ASME*) **74**:1 (2007), 81–99.

[Nemat-Nasser et al. 2007] S. Nemat-Nasser, W. J. Kang, J. D. McGee, W.-G. Guo, and J. B. Isaacs, "Experimental investigation of energy-absorption characteristics of components of sandwich structures", *Int. J. Impact Eng.* **34**:6 (2007), 1119–1146.

[Pai and Palazotto 2001] P. F. Pai and A. N. Palazotto, "A higher-order sandwich plate theory accounting for 3-D stresses", *Int. J. Solids Struct.* **38**:30–31 (2001), 5045–5062.

[Plantema 1966] F. J. Plantema, *Sandwich construction*, Wiley, New York, 1966.

[Vinson 1999] J. R. Vinson, *The behavior of sandwich structures of isotropic and composite materials*, Technomic, Lancester, PA, 1999.

Received 17 May 2009. Revised 23 Jun 2009. Accepted 9 Jul 2009.

RENFU LI: renfu.li@mail.hust.edu.cn
Department of Aerospace Engineering, Georgia Institute of Technology, Atlanta, GA 30332-0150, United States
Current address: *School of Energy and Power Engineering, HuaZhong University of Science and Technology, Wuhan 430074, China*

GEORGE KARDOMATEAS: george.kardomateas@aerospace.gatech.edu
Department of Aerospace Engineering, Georgia Institute of Technology, Atlanta, GA 30332-0150, United States